JOURNAL OF COLLOID AND INTERFACE SCIENCE 171, 470–473 (1995)

Analysis of Fractal Cluster Morphology Parameters: Structural Coefficient and Density Autocorrelation Function Cutoff

JIAN CAI, NINGLONG LU, AND CHRISTOPHER M. SORENSEN[1]

Physics Department, Kansas State University, Manhattan, Kansas 66506-2601

Received June 21, 1994; accepted October 27, 1994

Electron micrograph images of fractal soot clusters obtained from a premixed CH_4/O_2 flame are analyzed for two, somewhat neglected, morphological parameters: the structural coefficient k_0 in $N = k_0(R_g/a)^{D_f}$ and the perimeter cutoff function $h(x)$ of the cluster density autocorrelation function. We find for our fractal aggregates that $k_0 = 1.23 \pm 0.07$ and $h(x)$ is well described by a Gaussian or overlapping spheres model.

Key Words: fractal clusters; morphology; soot.

1. INTRODUCTION

The process of aggregation in colloids and aerosols leads to random aggregates of small primary particles. These aggregates have been shown to be describable by a fractal morphology (1–3); that is, the number of monomers per aggregate N scales with the radius of gyration R_g as

$$N = k_0\left(\frac{R_g}{a}\right)^{D_f}, \qquad [1]$$

where k_0 is a structural coefficient, a is the monomer radius, and D_f is the fractal dimension of the aggregate. Such a fractal description of the seemingly random structure brought about a major breakthrough in the study of aggregation phenomena. Much effort has been spent in studying the fractal dimension, which is of great importance in ramified aggregate morphology. A less well-studied parameter is the structural coefficient k_0. So far there is no general agreement as to the value of k_0, which is essential to fully characterize the morphology, nor have there been any systematic studies regarding the dependence of k_0 on the aggregation process.

We first realized the importance of k_0 during our light scattering studies of fractal soot aggregates, wherein we argued that k_0 can be determined by the $N \to 1$ limit of Eq. [1] (4). Computer simulations provide a means by which k_0 may be determined. Wu and Friedlander (WF) (5) gathered previously published simulation data and found k_0 ranged from 1.05 to 1.59 for diffusion limited cluster aggregation (DLCA) clusters and $k_0 \sim 1.3$ for these clusters in the free molecular regime, i.e., when the cluster radius is much less than the medium gas molecule mean free path. Another value for simulated smoke clusters was reported by Mountain and Mulholland (6), who gave $k_0 = 1.55$. Experimental methods of determining k_0 are also possible through transmission electron microscopy (TEM) or light scattering (7, 8). Puri *et al.* (7) reported from TEM analysis that $k_f \simeq 9.0$ and $D_f \simeq 1.4$, where $k_f = 2^{D_f}k_0$, since monomer diameter was used in their formula while we used monomer radius. With $D_f \simeq 1.4$, one finds $k_0 = 3.4$. Köylü and Faeth obtained $k_f = 8.1$ and $D_f = 1.82$ from their optical measurement (8), which gives $k_0 \simeq 2.3$. Both of these values are much bigger than those from simulations.

Another important morphological parameter is the cutoff function for the cluster density autocorrelation function $g(r)$, which is a power law function of the position variable r as a consequence of the scaling in Eq. [1],

$$g(r) \sim r^{D_f-d}, \qquad [2]$$

where d is the spatial dimension. The Fourier transform of this function gives the optical structure factor $S(q)$ for the scattered intensity, assuming that there is no intracluster multiple scattering. Here $q = 4\pi\lambda^{-1}\sin\theta/2$ is the magnitude of the scattering wave vector. The structure factor $S(q)$ also displays a scaling behavior for $qR_g \gg 1$ as

$$S(q) \sim q^{-D_f}, \qquad [3]$$

which signifies a fractal structure and is often used to determine the fractal dimension.

Equation [3] is very useful if sufficiently large q data are available and all that is desired is D_f. On the other hand, the complete expression for $S(q)$ for all q is necessary for analysis of data limited to $qR_g \leq 5$, since the asymptotic nature displayed in Eq. [3] is no longer present. The manner in which $S(q)$ transforms from the Rayleigh regime, where it is a constant, to the behavior in Eq. [3], i.e., the range $0 \leq qR_g \leq 5$, is determined by the large r behavior of $g(r)$.

[1] To whom correspondence should be addressed.

0021-9797/95 $6.00

There is an upper limit to the power law scaling in Eq. [2] and this upper limit is naturally the maximum cluster size. At the cluster perimeter, $g(r)$ will eventually fall to zero. Therefore we need a function to properly account for this cutoff behavior at the cluster edge: a cutoff function $h(x)$. Then the density autocorrelation function becomes

$$g(r) = Ar^{D_f-d}h(x), \qquad [4]$$

where A is a normalization constant and $x = r/\xi$ is dimensionless, with ξ being a characteristic length of the cluster. A knowledge of the correct cutoff function will let us determine $S(q)$ for all q.

Although the cutoff function for the density autocorrelation function has not been given much attention, the existing work from computational (6, 10, 11) studies indicates that the exponential cutoff, which is widely used (12–14), is not sharp enough. We (15) found from our light scattering data that the Gaussian cutoff function worked best for soot clusters, which is in good agreement with the computer simulations. One physical mechanism for the cutoff function may be obtained by considering two overlapping spheres (OS) (16, 17). The structure factor derived from the OS cutoff function is about the same as that from the Gaussian cutoff function (15).

Thus we conclude that a complete picture of fractal morphology should include k_0 and $h(x)$ as well as D_f. In this paper we report our results for k_0 and the cutoff function determined directly from TEM analysis of soot clusters collected from a premixed CH_4/O_2 flame.

2. EXPERIMENT

The procedure for creating, capturing, and analyzing soot clusters is the same as that used previously (18). The flame used was a premixed CH_4/O_2 flame with a carbon to oxygen atomic ratio of 0.75. The soot from this flame consists of DLCA fractal aggregates with $D_f = 1.79 \pm 0.1$, $a = 12$ nm, and $R_g \leq 150$ nm. The mean free path of the gas molecules in the flame is ca. 350 nm. To collect soot particles from the flame, we used a thermophoretic soot sampling device (19) which carried vertically oriented Formvar-coated copper TEM grids into and out of the flame at a height of either 12 or 18 mm above the burner surface. The entrance and exit times were ~5 ms and the residence time in the flame was ~15 ms. The grids were then examined with a TEM, and soot pictures were taken at the center of the grid with a magnification of 19,200.

The final soot prints, enlarged by a factor of 2, were scanned into PCX format files in 16 shades of gray using an Niscan scanner. The picture resolution used was 0.2 mm per pixel or 125 dpi (dot per inch). Considering the magnification of the picture, this resolution was equivalent to 5.2 nm per pixel, which was less than the size of a monomer. Each cluster from the ensemble was then "cut" and put into a separate file. This file was edited with a graphics editor to carefully remove all unwanted dark spots in the picture background not belonging to a cluster in order to get a clean picture of the soot cluster; that is, all background was white and only sites occupied by the cluster were dark (15 levels of different shades).

3. RESULTS

A major problem in TEM analysis of soot morphology is that one deals with two-dimensional projection of the three-dimensional clusters (18, 20, 21). The information regarding the third dimension may be lost. Our 16-shade formatted soot images, however, retain some, although not all, of the information of the third dimension. Our previous analysis showed that (18)

$$R_{g,2} = R_g \qquad [5]$$

$$D_2 \propto \text{cluster projected area} \qquad [6]$$

$$D_{16} \propto \text{cluster monomer number}, \qquad [7]$$

where $R_{g,2}$ is the R_g calculated from a 2-shade format, D_2 is the total darkness of the image obtained with a 2-shade format, and D_{16} is the total darkness of the image obtained with a 16-shade format. The 2-shade format is obtained from the 16-shade format by setting all nonzero shades, i.e., parts of the cluster, to one, and leaving all zero shades zero.

Our previous work (18) yielded good agreement between our TEM and light scattering results for R_g, D_f, N, and a; hence we have confidence in our micrograph analysis. From the TEM images, k_0 and $h(x)$ can be easily obtained.

1. k_0

R_g, N, D_f, and a were all determined in our previous analysis (18) for an ensemble of 92 clusters. A plot of N versus R_g/a for all the data on a log–log scale is shown in Fig. 1. The slope and intercept of the plot yielded $D_f = 1.74 \pm 0.04$ and $k_0 = 1.23 \pm 0.07$. This latter value is in good agreement with the $k_0 \sim 1.3$ listed in WF. The results from DLCA simulations done in this lab (to be published) gave $k_0 = 1.2 \pm 0.1$, which is in excellent agreement with our TEM analysis.

2. *Cutoff Function h(x)*

The cutoff function was obtained from the density autocorrelation function by inverting Eq. [4],

$$h(r) = A^{-1}g(r)r^{d-D_f}, \qquad [8]$$

where $d = 2$ for the 2-shade format and $d = 3$ for the 16-shade format. $g(r)$ was calculated from the digitized image

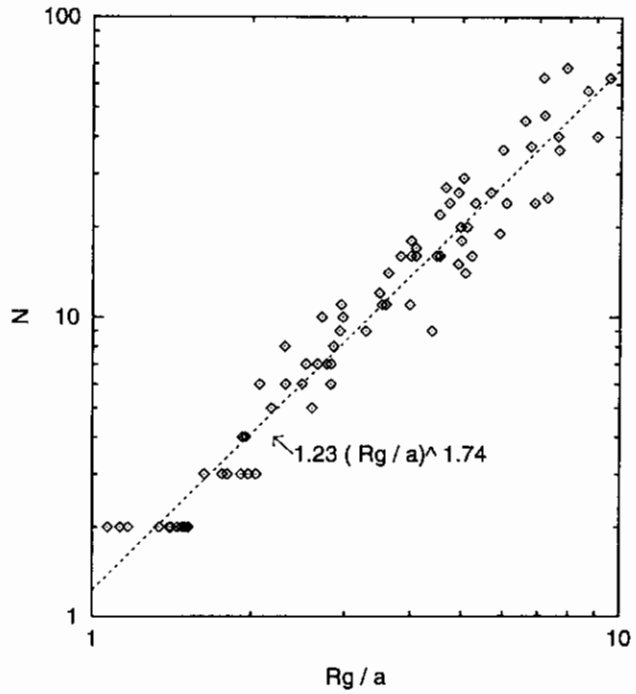

FIG. 1. Plot of N versus R_g/a for an ensemble of 92 clusters. The fit line slope gives $D_f = 1.74 \pm 0.04$ and the intercept yields $k_0 = 1.23 \pm 0.07$.

of the soot cluster by an algorithm similar to that in Samson *et al.* (22). From the $g(r)$, D_f was determined and used in the calculation of $h(r)$.

Figure 2 shows the cutoff function for four of the largest soot clusters. We have found that the projection into two dimensions has little effect for large clusters (18), so the two-shade format was used here.

Also plotted on the graph are the exponential cutoff function

$$h(r/\xi) = e^{-r/\xi}, \qquad [9]$$

where

$$\xi^2 = \frac{2}{D_f(D_f+1)} R_g^2; \qquad [10]$$

the Gaussian cutoff function

$$h(r/\xi) = e^{-(r/\xi)^2}, \qquad [11]$$

with

$$\xi^2 = \frac{4}{D_f} R_g^2; \qquad [12]$$

and the OS cutoff function

$$h(r/\xi) = (1 + x/4)(1 - x/2)^2, \qquad [13]$$

where $x = r/\xi$ and

$$\xi^2 = \frac{(D_f+2)(D_f+5)}{2D_f(D_f+1)} R_g^2; \qquad [14]$$

all for $D_f = 1.75$.

4. DISCUSSION AND CONCLUSION

Our measured value of $k_0 = 1.23 \pm 0.07$ from the TEM analysis is in good agreement with those from computer simulations listed in WF ($k_0 \sim 1.3$) and those obtained in this lab ($k_0 = 1.2 \pm 0.1$) (to be published), but it is much smaller than the experimental results of Puri *et al.* (7) and Köylü and Faeth (8). We do not know the reason for this discrepancy. Since this value, as determined from an ensemble of clusters, is an average, it may depend on the size range from which it is determined.

In earlier work (15) we used light scattering data fitted to various structure factors derived from different forms of the cutoff function in order to obtain D_f and found that the exponential cutoff function performed badly and by no means could yield results compatible with D_f as reported from previous experiments and simulations for a flame system. We remark that this structure factor is well represented by the so-called Fisher–Burford form. On the other hand,

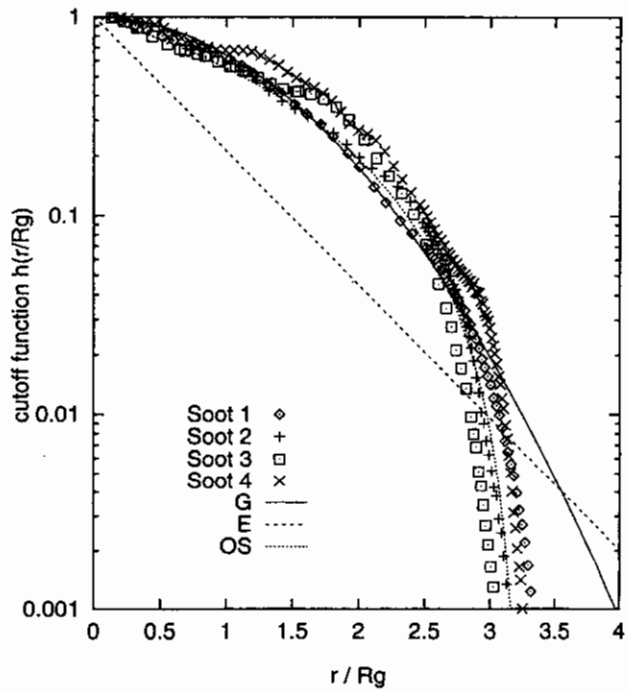

FIG. 2. Plot of the cutoff function $h(x)$ for the four largest clusters and of the exponential (E), Gaussian (G), and overlapping spheres (OS) cutoff functions. The cutoff functions of the soot clusters are in excellent agreement with the Gaussian and the OS cutoff functions.

the Gaussian cutoff function did a good job of fitting the data when polydispersity was included. It is clearly seen that the soot cutoff functions from TEM analysis agree very well with the Gaussian cutoff function up to $r = 3R_g$. No agreement with the exponential cutoff function is seen. The OS cutoff function yields the best comparison, dropping to zero at about the same r/R_g value as that of the soot cutoff. Therefore this result lends further support to our light scattering result that the exponential cutoff function is not sharp enough to do an adequate job in describing the cluster perimeter cutoff and a structure factor similar to the one derived from the OS or Gaussian cutoff function is the appropriate one for soot clusters.

We note that for $r \geqslant 3R_g$ the soot cutoff functions from TEM analysis begin to fall much more sharply than the Gaussian cutoff function. This should be so for a real cluster since the cutoff function goes to zero at $r = l_{max}$, where l_{max} is the maximum length of the cluster. Our data gave $l_{max} = 3.18$–$3.52\ R_g$, with an average of $l_{max} = 3.33R_g$. For $D_f = 1.75$, the OS cutoff function falls to zero at $l_{max} = 3.24R_g$, which agrees well with the soot particles. Although the Gaussian cutoff function will not go to zero until ∞, the extra tail is small and only adds a negligible uncertainty to the derived structure factor. From a physical point of view, the OS cutoff best describes the cluster. However, it is more difficult to use in performing a fit since it does not yield an analytical form for the structure factor for a noninteger D_f. From a calculation point of view, the Gaussian cutoff is preferred because it yields an analytical structure factor (15) which is about the same as the OS structure factor.

ACKNOWLEDGMENT

This work was supported by NSF Grant CTS 9024668.

REFERENCES

1. Forrest, S. R., and Witten, T. A., *J. Phys. A* **12,** L109 (1979).
2. Family, F., and Landau, D. P. (Eds.), "Kinetics of Aggregation and Gelation." North-Holland, Amsterdam, 1984.
3. Stanley, H. E., and Ostrowsky, N. (Eds.), "On Growth and Form." Nijhoff, Boston, 1986.
4. Sorensen, C. M., Cai, J., and Lu, N., *Appl. Optics* **31,** 6547 (1992).
5. Wu, M. K., and Friedlander, S. K., *J. Colloid Interface Sci.* **159,** 246 (1993).
6. Mountain, R. D., and Mulholland, G. W., *Langmuir* **4,** 1321 (1988).
7. Puri, R., Richardson, T. F., Santoro, R. J., and Dobbins, R. A., *Combust. Flame* **92,** 320 (1993).
8. Köylü, Ü. Ö., and Faeth, G. M., *J. Heat Transfer* **116,** 152 (1994).
9. Gangopadhyay, S., Elminyawi, I., and Sorensen, C. M., *Appl. Optics* **25,** 4859 (1991).
10. Nelson, J., *J. Mod. Opt.* **36,** 1031 (1989).
11. Lin, M. Y., Klein, R., Lindsay, H. M., Weitz, D. A., Ball, R. C., and Meakin, P., *J. Colloid Interface Sci.* **137,** 263 (1993). [Note that the structure factor for the exponential cutoff is misplotted in Fig. 2]
12. Berry, M. V., and Percival, I. C., *Opt. Acta* **33,** 577 (1986).
13. Freltoft, T., Kjems, J. K., and Sinha, S. K., *Phys. Rev. B* **33,** 269 (1986).
14. Teixeira, J., *in* "On Growth and Form" (H. E. Stanley and N. Ostrowsky, Eds.). Nijhoff, Boston, 1986.
15. Sorensen, C. M., Cai, J., and Lu, N., *Langmuir* **8,** 2064 (1992).
16. Glatter, O., and Kratky, O., "Small Angle X-Ray Scattering." Academic Press, New York, 1982.
17. Hurd, A., and Flower, W. L., *J. Colloid Interface Sci.* **122,** 178 (1988).
18. Cai, J., Lu, N., and Sorensen, C. M., *Langmuir* **11,** 2861 (1993).
19. Dobbins, R. A., and Megaridis, C. M., *Langmuir* **3,** 254 (1987).
20. Megaridis, C. M., and Dobbins, R. A., *Combust. Sci. Technol.* **71,** 95 (1990).
21. Weitz, D. A., and Huang, J. S., *in* "Kinetics of Aggregation and Gelation" (F. Family and D. P. Landau, Eds.). North-Holland, Amsterdam, 1984.
22. Samson, R. J., Mulholland, G. W., and Gentry, J. W., *Langmuir* **3,** 272 (1987).